IEEE Access
Multidisciplinary | Rapid Review | Open Access Journal

Received 13 December 2023, accepted 8 January 2024, date of publication 11 January 2024, date of current version 22 January 2024.

Digital Object Identifier 10.1109/ACCESS.2024.3352647

RESEARCH ARTICLE

Event-Triggered Robust Optimal Control for PMSM With Unknown Internal Dynamics, Disturbances, and Constrained Inputs

LUY NGUYEN TAN[1], (Senior Member, IEEE), THANH PHAM CONG[2], AND DUY PHAM CONG[3]

[1]Faculty of Electric-Electronics Engineering (FEEE), Ho Chi Minh City University of Technology (HCMUT), Vietnam National University Ho Chi Minh City (VNU-HCM), Ho Chi Minh City 700000, Vietnam
[2]Vietnam Aviation Academy, Ho Chi Minh City 712100, Vietnam
[3]Faculty of Electrical Engineering Technology, Industrial University of Ho Chi Minh City, Ho Chi Minh City 700000, Vietnam

Corresponding author: Luy Nguyen Tan (ntanluy@hcmut.edu.vn)

ABSTRACT In industry, for driving a permanent magnet synchronous motor (PMSM), it is more favorable to optimize control performances and reduce computational complexity and communication waste from a controller to actuators. For that reason, this paper employs an event-triggering mechanism to design a robust optimal control strategy for PMSM. Firstly, the PMSM model is presented as a strict-feedback nonlinear system with unknown internal dynamics, disturbances, and constrained inputs. Then, an event-triggered (ET) feedforward control strategy is introduced to convert the separated speed and current dynamics into an augmented system. Secondly, an ET-robust optimal feedback control strategy and an ET disturbance compensation strategy are designed using adaptive dynamic programming (ADP) and zero-sum game theory. All controller parameters are tuned online without identifying unknown dynamics or using a persistent excitation condition. It is shown that system stability and the exclusion of Zeno's behavior are fulfilled. Finally, compared with the existing time-triggering control strategies in simulation and experiments with TMS320F28335 of Texas Instruments, the proposed strategy is more effective in reducing the burden of computation bandwidth and communication load.

INDEX TERMS PMSM drives, event-triggering, optimal control, input constraints, disturbances, drift parameters.

I. INTRODUCTION

PMSM is the most popular alternating current (AC) actuator developed for industrial applications such as electric vehicles, conveyor belts, wind turbines, etc. Improvements in its control performance have constantly attracted the attention of the control community [1], [2], [3], [4], [5]. In most control strategies, conventional time-driven control has been used, known as time-triggered control strategies with a fixed sampling period. In operation, controllers update parameters periodically based on an initially fixed sampling rate, regardless of whether the parameters require updating or not. In other words, the burden of computational bandwidth and communication load from the controllers to PMSM drives has not been evaluated.

In a field-oriented control scheme, the control performance, especially during the transient condition, is dependent on the sampling rates of the speed and current loops in a *dq* reference frame [1]. The sampling time depends on the switching frequency, which is often high, leading to a high periodic update frequency for the controller. In most situations, although the reference speed and torque disturbance do not change, the speed and current controllers continuously compute and send to inverters the same control voltages as the previous signal sequence.

Recently, the event-triggering mechanism [6] has been applied to design control strategies that update parameters, generate, and send new control signals to actuators only

The associate editor coordinating the review of this manuscript and approving it for publication was Jiefeng Hu.

when new events occur; otherwise, they stop updating and transfer the previous control signals using zero-order holders (ZOH). The ET control policies have been proven to be effective for linear and nonlinear systems [7], [8] with industrial applications [9], [10]. Sahoo et al. [7] employed the event-triggering principle and game theory to design a control scheme with disturbance rejection for linear systems. Zhang et al. [8] proposed an event-triggered optimal strategy with disturbance rejection for nonlinear systems. The event-triggering mechanism was embedded into the actor-critic control schemes to create optimal control laws for the heating, ventilation, and air conditioning systems [9] and for macro–micro composite stage systems [10]. However, in the works mentioned above, input constraints are not considered. Recently, Yang et al. [11] have proposed an ADP algorithm for uncertain underactuated mechatronic systems with actuator constraints. By employing the Lyapunov function candidate appropriately, tracking performance with asymptotic stability rather than uniformly ultimate bounded (UUB) stability is obtained. However, the event-triggering mechanism is not integrated into the algorithm to mitigate the communication load between the actuators and controllers.

For PMSM drives, few studies have dealt with ET control strategies. Wang et al. [12] designed an event-triggered and back-stepping-based control scheme with known dynamics subject to limited communication bandwidth and mismatched disturbances. Zhou et al. [13] proposed a finite-time adaptive ET output feedback control scheme using neural networks. The scheme can be applied to PMSM systems with unknown nonlinear dynamics and immeasurable states. In [14], the ET control scheme can be applied to the position tracking control, where a dynamic gain is employed to deal with sampling errors and uncertainties due to unknown time-varying torques. Although the existing schemes related to the event-triggering mechanism have many advantages when applied to PMSM systems, they have not yet been developed for optimal control strategies to minimize the cost functions.

It is worth emphasizing that the object of PMSM control design is not only stability but also optimization. The design needs to create stable controllers for closed loops of speed and current along with optimization of a cost function. In [4], [5], optimal controllers, which minimize horizontal quadratic cost functions, are obtained by solving Riccati equations. In [15], by considering PMSM as a linear model, the algorithms are designed to minimize the quadratic cost functions of the currents with constrained dq-axis control inputs. However, the designs relied on linear models and Riccati equations cannot deal with the external disturbances or uncertain parameters.

In industrial applications, the constraints of dq-axis control inputs are required to keep amplitude modulation indices limited in linear ranges [2], [16]. In [17], an optimal control method dealing with saturated control voltages and torque disturbances is proposed, where conventional cascade proportional-integral (PI) control loops are integrated into a single loop. Then, a horizontal $\mathcal{H}_\infty$ performance index function is minimized by an $\mathcal{H}_\infty$ optimal controller. In addition, in this method, internal dynamics knowledge does not need to be acquired.

Most of the optimal control methods mentioned above have not exploited the strengths of the event-triggering mechanism in reducing the computational bandwidth and communication waste for industrial PMSM drives. Adopting the existing event-triggering strategies for optimal control has to face some challenges: *i*) PMSM dynamics are separated by current and speed in the presence of drift parameters, constrained inputs, and external disturbances [17], to which the existing ET optimal control methods for affine systems [7], [9], [10], [12], [14], [18] cannot be applied. *ii*) Designing an ET control strategy for the separated current and speed dynamics, which are inherently unstable in the inter-event intervals, is difficult. *iii*) The persistent excitation (PE) condition, required for parameter convergence [19], is impossible to verify online in event-triggering practice.

To address the challenges mentioned, robust optimal control is proposed in this paper. To the best of our knowledge, this is the first time an event-triggering mechanism has been integrated into a ADP control scheme for PMSM drives. The main contributions are described as follows:

1) PMSM models are presented by a strict-feedback nonlinear system with unknown internal dynamics, disturbances, and constrained inputs in two loops of speed dynamics and current dynamics. Since the dynamics possess separate loops, they are transformed into an augmented system by an ET-feedforward control strategy.
2) Unlike existing ADP algorithms for PMSMs [17], the new ADP control algorithm in the paper, which integrates the event-triggering mechanism, can reduce computational bandwidth and communication waste between controllers and PMSM drivers. The control scheme can approximate the ET-robust optimal control (ETROC) strategy together with the ET disturbance compensation strategy. The gradient of the Hamilton-Jacobi-Isaacs (HJI) solution is estimated for the strategies by a simple online approximator. An event-triggering condition is introduced to reduce the number of samples and maintain the stability of the closed-loop system. To deal with unknown internal dynamics, the integral reinforcement learning (IRL) technique is employed. To ensure the relaxation of PE conditions and fast convergence of the parameters, the approximator tuning law is derived by mining past feedback data.
3) A UUB stability analysis of the tracking and approximation errors is implemented. In addition, the Zeno phenomenon is proven to be excluded. Compared with the existing time-triggering control strategies in simulation and experiments onboard the TI TMS320F28335, the number of controller parameter updates for the proposed strategy is much smaller.

In the following, Section II designs an ET-feedforward control strategy, Section III proposes an ET-robust optimal control strategy, and Section IV conducts a simulation and experiment. Finally, Section V comes to a conclusion.

II. SYSTEM AND ET-FEEDFORWARD CONTROL

A. PMSM MODELS IN STRICT-FEEDBACK FORM

Consider PMSM models represented by strict-feedback nonlinear systems with unknown internal dynamics, constrained inputs, and external disturbances as

$$\begin{cases} \dot{x}_\omega = f_\omega(x_\omega) + k_\omega(x_\omega) d_\omega, \\ \dot{x}_i = f_i(x_\omega, x_i) + g_i(x_\omega, x_i) v + d_i, \end{cases} \tag{1}$$

where n_p is a number of pole pairs, $x_i = [x_{i_d}, x_{i_q}]^\top$, $x_{i_d} = i_d$, $x_{i_q} = i_q$ are stator currents in the dq-axis, $x_\omega = \omega$, ω is mechanical rotor speed, $v = [v_d, v_q]^\top$, v_d and v_q are control inputs bounded by λ because of power converter voltage limits, where $|v_d| \le \lambda$, $|v_q| \le \lambda$, L_d, L_q are the stator inductance in dq-axis, R_s is stator resistance, d_ω, $d_i = [d_d, d_q]^\top$, T_L, B are load torque disturbance, current disturbances, load torque, and viscous friction coefficient, respectively. For permanent magnet flux linkage ψ_f, moment of inertia J, denote $k_\omega(x_\omega) = \frac{1}{J}$,

$$g_\omega(x_\omega) = \begin{bmatrix} 0 & \dfrac{1.5 n_p \psi_f}{J} \end{bmatrix}, g_i(x_\omega, x_i) = \mathrm{Diag}\left(\frac{1}{L_d}, \frac{1}{L_q}, \right),$$

and

$$\begin{cases} f_\omega(x_\omega) = -\dfrac{B}{J} x_\omega - \dfrac{T_L}{J}, \\ f_i(x_\omega, x_i) = \begin{bmatrix} -\dfrac{R_s}{L_d} x_{i_d} + n_p x_\omega x_{i_q} \\ -n_p x_\omega x_{i_d} - \dfrac{R_s}{L_q} x_{i_q} - \dfrac{n_p \psi_f}{L_q} x_\omega \end{bmatrix}, \end{cases}$$

where $f(x_\omega, x_\omega, x_i) = [f_\omega(x_\omega), f_i^\top(x_\omega, x_i)]^\top$ is internal dynamics. Parameters L_d, L_q, R_s, ψ_f, and J in internal dynamics $f(x_\omega, x_\omega, x_i)$ are assumed to be completely unknown in the design of the control scheme.

Remark 1: We represent PMSM dynamics (1) in strict-feedback nonlinear systems for facilitating the design of an optimal control scheme. The strict-feedback form will be converted to an affine form under the augmented control scheme proposed in the next section.

Remark 2: Load torque disturbances d_ω in (1) affecting motor speed need to be eliminated. These disturbances can be compensated by the estimated disturbances of a disturbance observer [3]. In addition, it is also necessary to remove the current disturbances d_d and d_q caused by the sensor measurement. In this paper, we approach $\mathcal{H}_\infty$ control methods to reject these disturbances.

Next, the boundedness and assumption are introduced to facilitate ET strategy design later:

Boundedness 1 ([20]): There exist positive constants $J_{\max}, g_{1\max}, g_{2\max}, b_\tau, b_d, b_q$ such that $\|k_\omega(x_\omega)\| = \|1/J\| \le J_{\max}$, $\|g_\omega(x_\omega)\| \le g_{1\max}$, $\|g_i(x_\omega, x_i)\| \le g_{2\max}$, $\|d_q\| \le b_q$, $\|d_\omega\| \le b_\tau$, $\|d_d\| \le b_d$.

Assumption 1: The desired angular velocity ω_d is bounded and smooth.

Definition 1 ([21]): For a bound $B > 0$, an equilibrium point x_0 of dynamics $\dot{x} = f(x), x \in \mathbb{R}^n$ is UUB in a compact set $\Omega \in \mathbb{R}^n$ if there exists $\|x - x_0\| \le B$, $x_0 \in \Omega$, $\forall t > t_0 + T(B, x_0)$.

B. ET-FEEDFORWARD CONTROL STRATEGY

To integrate two closed loops in (1) into an augmented system, we propose an ET-feedforward strategy. The design steps are built by using a standard back-stepping procedure [22] and an event-triggering mechanism [6].

Step 1: Given a sequence of monotonically increasing aperiodic instants $\{t_0, t_1, \ldots, t_k, t_{k+1}, \ldots\}$, let some signals be sampled at t_k and kept until $t_{k+1}, k = 0, 1, \ldots$, the speed and currents from dynamics (1) are changed to new coordinates as

$$\begin{cases} z_\omega(t) = x_\omega(t) - \omega_d(t), \\ z_i(t) = x_i(t) - \underline{x}_i^{d(t)}, \end{cases} \tag{2}$$

where $\underline{x}_i^d(t) = [\underline{x}_{i_d}^d, \underline{x}_{i_q}^d]^\top, t_k \le t < t_{k+1}$ are ET-virtual control inputs, to be designed in Step 3, sampled at t_k and kept until $t_{k+1}, k = 0, 1, \ldots, z_i = [z_{i_d}, z_{i_q}]^\top$.

Step 2: At a triggering instant $t_k, k = 0, 1, \ldots$, the speed and currents are sampled as $\underline{x}_\omega(t) = x_\omega(t_k)$, $\underline{x}_i(t) = x_i(t_k)$. Then, the triggering errors are defined as

$$e_h(t) = x_h(t) - \underline{x}_h(t), h = \omega, i, t_k \le t < t_{k+1}. \tag{3}$$

Step 3: At a triggering instant $t_k, k = 0, 1, \ldots$, introduce $\underline{x}_i^d(t)$ and the ET actual control inputs $\underline{v}(t)$ as

$$\begin{cases} \underline{x}_i^d(t) = \underline{x}_i^a(t) + \underline{x}_i^\star(t), \\ \underline{v}(t) = \underline{v}^a(t) + \underline{v}^\star(t), \end{cases} \tag{4}$$

where $\underline{v}(t) = v(t_k) = [\underline{v}_d \ \underline{v}_q]^\top$, $\underline{x}_i^a(t) = x_i^a(t_k) = [\underline{x}_{i_d}^a, \underline{x}_{i_q}^a]^\top$ and $\underline{v}^a(t) = v^a(t_k) = [\underline{v}_d^{a\star}, \underline{v}_q^{a\star}]^\top$ are ET-virtual and actual feedforward control vectors, $\underline{x}_i^\star(t) = x_i^\star(t_k) = [\underline{x}_{i_d}^\star, \underline{x}_{i_q}^\star]^\top$ and $\underline{v}^\star(t) = v^\star(t_k) = [\underline{v}_d^\star, \underline{v}_q^\star]^\top$ are ET-virtual and actual optimal control strategies designed later. All signals are updated at t_k and kept constant by a ZOH until t_{k+1}.

Step 4: Design $\underline{x}_i^a$ and $\underline{v}^a$ that satisfy the following constrains

$$\begin{cases} g_\omega(x_\omega) \underline{x}_i^a(t) = \dot{\underline{\omega}}_d(t) - \chi \underline{z}_\omega(t), \\ g_i(x_\omega, x_i) \underline{v}^a(t) = \dot{\underline{x}}_i^d(t) - \chi \underline{z}_i(t), \end{cases} \tag{5}$$

where $\dot{\underline{\omega}}_d(t) = \dot{\omega}_d(t_k)$ and $\dot{\underline{x}}_i^d(t) = \dot{x}_i^d(t_k)$.

Step 5: Design the triggering condition as

$$\|e_h(t)\| \le \kappa \|z_h(t)\|, \ h = \omega, i, \tag{6}$$

where $0 < \kappa \le \frac{b_g}{\chi}$, $b_g = \max(g_{1\max}, g_{2\max})$, $\chi \ge (2b_g + \frac{1}{4})$.

The stability of the transformed system using Steps 1 to 5 is analyzed through *Lemma* 1 as follows:

Lemma 1: Let the ET-virtual control inputs be defined in (4), the ET-feedforward control inputs $\underline{x}_i^a$ and $\underline{v}^a$ be given in (5), and assume there exist the feedback control inputs $\underline{x}_i^*$

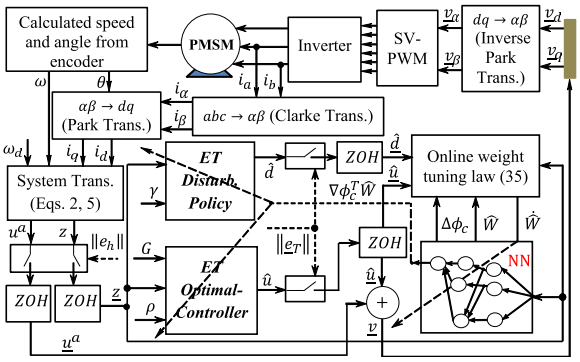

FIGURE 1. ET-robust optimal control structure for PMSM drives.

and $\underline{v}^*$ that stabilize the closed dynamics of the following augmented nonlinear system:

$$\begin{bmatrix}\dot{z}_\omega\\ \dot{z}_i\end{bmatrix}=\begin{bmatrix}f_\omega(x_\omega)\\ f_i(x_\omega,x_i)\end{bmatrix}+\begin{bmatrix}g_\omega(x_i) & 0_{1\times2}\\ 0_{2\times2} & g_i(x_\omega,x_i)\end{bmatrix}\begin{bmatrix}\underline{x}_i^\star\\ \underline{v}^\star\end{bmatrix}+\begin{bmatrix}k_\omega(x_\omega) & 0_{1\times2}\\ 0_{2\times1} & \mathrm{I}_{2\times2}\end{bmatrix}\begin{bmatrix}d_\omega\\ d_i\end{bmatrix}. \tag{7}$$

Then, the control problem of PMSM (1) is equivalent to the control problem of the augmented system (7).

Proof: See Appendix A. ■

Lemma 2 ([17], [23]): Let the ET-feedforward control inputs for (7) be bounded,

$$|\underline{u}_p^a|\le\lambda-\eta\tanh(1), p=\{i_d,i_q,d,q\}. \tag{8}$$

Let $\underline{u}_p^\star$ be a tanh function mapping $\mathbb{R}$ onto $(-\eta,\eta), 0<\eta\le\lambda$. Then, ET control inputs for (1) are still saturated, i.e., $|\underline{v}_d|\le\lambda$ and $|\underline{v}_q|\le\lambda$.

III. ET-ROBUST OPTIMAL CONTROL STRATEGY

By Lemmas 1 and 2, the ETROC strategy $\underline{u}^\star$ of the system (7) needs to be designed. We build an ET-robust optimal control structure (Fig. 1) with Park and Clarke basic transforms [16] and the ET optimal strategy and ET disturbance compensation policy, which are going to be designed in the following.

A. HAMILTON-JACOBI-ISACSS EQUATION

Consider (9) with drift parameters, constrained inputs and disturbances, we rewrite (7) in the affine dynamics as

$$\dot{z}=F(x)+G(x)\underline{u}^\star+K(x)d, \tag{9}$$

where $z=[z_\omega,z_i^\top]^\top$, $x=[x_\omega,x_i^\top]^\top$, $d=[d_\omega,d_i^\top]^\top$, $\underline{u}^\star=[\underline{x}_i^{\star\top},\underline{v}^{\star\top}]^\top$. Note that both ET-feedforward control inputs $\underline{u}^a=[\underline{x}_i^{a\top},\underline{v}^{a\top}]^\top$ and $\underline{u}^\star$ are constrained.

Based on the game theory in robust optimal control problem [24], we define an event-triggering value function

$$\mathcal{J}(\underline{z},\underline{d},\underline{u})=\int_t^\infty\left(\underline{z}^\top Q\underline{z}+U(\underline{u})-\gamma^2\underline{d}^\top\underline{d}\right)\mathrm{d}\tau, \tag{10}$$

where $Q\ge0$, $\underline{u}$ is an instant of $\underline{u}^\star$, $\underline{d}=d(t_k)$, $\gamma>0$ is the desired disturbance compensation factor. $U(\underline{u})$ is the nonnegative function, which can be chosen $U(\underline{u})=\underline{u}^\top R\underline{u}$ [24] in the unconstrained case, otherwise, according to Lemma 2, it is

$$U(\underline{u})=2\eta\int_0^{\underline{u}}\tanh^\top(s/\eta)R\mathrm{d}s, \tag{11}$$

where R is a positive definite diagonal matrix.

The Hamiltonian is formulated by

$$\mathcal{H}\left(\nabla\mathcal{J}(\underline{z}),\underline{z},\underline{d},\underline{u}\right)=r(\underline{z},\underline{d},\underline{u})+\nabla\mathcal{J}^\top(\underline{z})\left(F+G\underline{u}^\star+K\underline{d}\right), \tag{12}$$

where $r(\underline{z},\underline{d},\underline{u})=\underline{z}^\top Q\underline{z}+U(\underline{u})-\gamma^2\underline{d}^\top\underline{d}$, $\nabla\mathcal{J}(\underline{z})=\partial\mathcal{J}(\underline{z})/\partial\underline{z}$. Then, we can apply the zero-sum game theory [24] to obtain the ET optimal value:

$$\mathcal{J}^\star(\underline{z})=\max_{\underline{d}}\min_{\underline{u}}\int_0^\infty r(\underline{z},\underline{u},\underline{d})\mathrm{d}\tau. \tag{13}$$

Applying the stationary condition to (12), the ET disturbance compensation and the ET optimal control strategies, $\underline{d}^\star$ and $\underline{u}^\star$, are given by

$$\frac{\partial\mathcal{H}\left(\underline{z},\underline{u},\underline{d},\nabla\mathcal{J}^\star(\underline{z})\right)}{\partial\underline{d}}=0\Rightarrow\underline{d}^\star=\frac{1}{2\gamma^2}K^\top(\underline{x})\nabla\mathcal{J}^\star(\underline{z}), \tag{14}$$

$$\frac{\partial\mathcal{H}\left(\underline{z},\underline{u},\underline{d},\nabla\mathcal{J}^\star(\underline{z})\right)}{\partial\underline{u}}=0\Rightarrow\underline{u}^\star=-\eta\tanh(M^\star), \tag{15}$$

where $\underline{x}=x(t_k), k=0,1,\ldots, M^\star=\frac{1}{2\eta}R^{-1}G^\top(\underline{x})\nabla\mathcal{J}^\star(\underline{z})$. Using the Hamiltonian (12), (14) and (15), the equation HJI is written as

$$\begin{aligned}\mathcal{H}^\star\left(\nabla\mathcal{J}^\star(\underline{z}),\underline{z},\underline{d}^\star,\underline{u}^\star\right)&=\nabla\mathcal{J}^{\star\top}(\underline{z})\left(F+G\underline{u}^\star+K\underline{d}^\star\right)\\&\quad+\underline{z}^\top Q\underline{z}+U(\underline{u}^\star)-\gamma^2\underline{d}^{\star\top}\underline{d}^\star=0.\end{aligned} \tag{16}$$

According to [25], the minimal positive definite smooth values of a solution $\mathcal{J}^\star(\underline{z})$ to HJI (16) always exists but cannot solve analytically. The solution is therefore approximated by an approximation function combined with an event-triggering mechanism regarding the high-order nonlinear differential of HJI with drift parameters.

B. FUNCTION APPROXIMATION FOR ETROC STRATEGY

Inspired by the Weierstrass theorem of function approximation [26], [27], for activation functions $\varphi(\underline{z}):\mathbb{R}^3\to\mathbb{R}^n$, ideal weights $W\in\mathbb{R}^n$, and approximation errors $\varepsilon(\underline{z})$, we can represent $\mathcal{J}^\star(\underline{z})$ as

$$\mathcal{J}^\star(\underline{z})=W^\top\varphi(\underline{z})+\varepsilon(\underline{z}), \tag{17}$$

where $\varphi(\underline{z})$ satisfies the following assumption.

Assumption 2 ([26], [27]): For a complete independent basis set $\varphi(\alpha)$, $\forall\alpha\in\mathbb{R}^3$ and some positive constants $b_\varphi, b_{\nabla\varphi}$, $b_\varepsilon, b_{\nabla\varepsilon}$, the following bounds are satisfied: $\|\varphi(\alpha)\|\le b_\varphi$, $\|\nabla\varphi(\alpha)\|=\|\frac{\partial\varphi(\alpha)}{\partial\alpha}\|\le b_{\nabla\varphi}$, $\|\nabla\varepsilon(\alpha)\|=\|\frac{\partial\varepsilon(\alpha)}{\partial\alpha}\|\le b_{\nabla\varepsilon}$, $\|\varepsilon(\alpha)\|\le b_\varepsilon$. In addition, for a positive constant $L_{\nabla\varphi}$, $\nabla\varphi(\alpha)$ is Lipschitz:

$$\left\|\nabla\varphi(z)-\nabla\varphi(\underline{z})\right\|\le L_{\nabla\varphi}\left\|z-\underline{z}\right\|=L_{\nabla\varphi}\left\|\underline{e}\right\|. \tag{18}$$

Due to unknown weights, $\mathcal{J}^\star(\underline{z})$ is approximated by

$$\hat{\mathcal{J}}(\underline{z}) = \hat{W}^\top \varphi(\underline{z}). \tag{19}$$

Then, the strategies of the optimal control and disturbance compensation are approximated by

$$\hat{\underline{u}} = -\eta \tanh(\hat{M}),\ \hat{M} = \frac{1}{2\eta} R^{-1} G^\top \nabla \hat{\mathcal{J}}(\underline{z}), \tag{20}$$

$$\hat{\underline{d}} = \frac{1}{2\gamma^2} K^\top \nabla \hat{\mathcal{J}}(\underline{z}). \tag{21}$$

From (20) and (21), the dynamics (7) can be rewritten as

$$\dot{z} = F + G\hat{\underline{u}} + K\hat{\underline{d}}. \tag{22}$$

Then, the HJI (16) becomes

$$\begin{aligned}\hat{\mathcal{H}} = \hat{W}^\top \nabla\varphi(\underline{z}) \left(F + G\hat{\underline{u}} + K\hat{\underline{d}}\right) \\ + \underline{z}^\top Q \underline{z} + U(\hat{\underline{u}}) - \gamma^2 \hat{\underline{d}}^\top \hat{\underline{d}}.\end{aligned} \tag{23}$$

From (16)-(23), it can be seen that if $\lim_{t\to\infty} \|\hat{\mathcal{H}}(t) - \mathcal{H}^\star(t)\| = 0$, then $\hat{W} \to W$. Followed by the IRL technique [28], the squared residual error is defined $E_{\hat{H}} = \frac{1}{2} e_{\hat{\mathcal{H}}}^\top e_{\hat{\mathcal{H}}}$, where

$$e_{\hat{\mathcal{H}}} = \hat{W}^\top \Delta\varphi(t) + \int_{t-T}^{t} \hat{r} \mathrm{d}\tau, \tag{24}$$

where $\hat{r} = \underline{z}^\top Q \underline{z} + U(\hat{\underline{u}}) - \gamma^2 \hat{\underline{d}}^\top \hat{\underline{d}}$, and

$$\begin{aligned}\Delta\varphi(t) &= \int_{t-T}^{t} \nabla\varphi(z) \left(F + G\hat{\underline{u}} + K\hat{\underline{d}}\right) \mathrm{d}\tau\tau \\ &= \int_{t-T}^{t} \nabla\varphi(z) \dot{z} \mathrm{d} = \varphi(t) - \varphi(t-T).\end{aligned} \tag{25}$$

To ensure the relaxation of PE condition and the parameter convergence to global values, we employ the concurrent learning technique [29], where we require the minimization of the objective function of past errors, $E_p = \sum_{l=1}^{P} E_{\hat{H}}(t_l)$, $E_{\hat{H}}(t_l) = \frac{1}{2} e_{\hat{H}}^\top(t_l) e_{\hat{H}}(t_l)$, where

$$e_{\hat{H}}(t_l) = \hat{W}^\top \Delta\varphi(t_l) + \int_{t_l-T}^{t_l} \hat{r} \mathrm{d}\tau, \tag{26}$$

where $\Delta\varphi(t_l)$, $\hat{r}(t_l)$ at $t_l = \{t_0, t_1, \ldots, t_P\} < t$ are stored in sets $\{\Delta\varphi(t_l)\}_{l=1}^{P}$, $\{\hat{r}(t_l)\}_{l=0}^{P}$. The size of the set satisfies the condition of the concurrent learning:

Condition 1 ([29]): $\mathrm{rank}[\Delta\varphi(t_0), \Delta\varphi(t_1), \ldots, \Delta\varphi(t_P)] = P$.

From the gradient descent rule, for an update rate $\beta > 0$, we design a NN weight-tuning law, such that $\dot{\hat{W}} = -\beta \frac{\partial E_{\hat{H}}}{\partial \hat{W}} - \beta \sum_{l=1}^{P} \frac{\partial E_{\hat{H}}(t_l)}{\partial \hat{W}}$, i.e.,

$$\begin{aligned}\dot{\hat{W}} = -\beta \Delta\varphi \Delta\varphi^\top \hat{W} - \beta \Delta\varphi \int_{t-T}^{t} \hat{r}(\tau) \mathrm{d}\tau \\ - \beta \sum_{l=1}^{P} \Delta\varphi(t_l) \left(\Delta\varphi^\top(t_l) \hat{W} + \int_{t_l-T}^{t_l} \hat{r}(\tau) \mathrm{d}\tau\right).\end{aligned} \tag{27}$$

Define $\tilde{W} = W - \hat{W}$, approximation error dynamics is written as

$$\begin{aligned}\dot{\tilde{W}} = -\beta \sum_{l=1}^{P} \Delta\varphi(t_l) \left(\Delta\varphi^\top(t_l) \tilde{W} - \varepsilon_H(t_l)\right) \\ - \beta \Delta\varphi \left(\Delta\varphi^\top \tilde{W} - \varepsilon_H\right),\end{aligned} \tag{28}$$

where $\varepsilon_H(t_l) := \int_{t_l-T}^{t_l} \nabla\varepsilon^\top \dot{z} \mathrm{d}\tau$, which is upper bounded by $\sup_{t_l>0} \|\varepsilon_H(t_l)\| \le b_{\varepsilon H}$.

Condition 2 (Event-triggering condition): The control strategy needs a triggering law that satisfies $\|\underline{e}\| < \sqrt{\|\underline{e}_T\|}$. We design a triggering threshold $\underline{e}_T$ as

$$\underline{e}_T = (1-\alpha) \frac{(1-\eta)\lambda_{\min}(Q) \|\underline{z}\|^2 + U(\hat{\underline{u}}) - \gamma^2 \|\hat{\underline{d}}\|^2}{\left(\frac{1}{\eta} - 1\right)\lambda_{\min}(Q) + L^2 \|R^{-1}\| \|\hat{W}\|^2}, \tag{29}$$

where $0 < \eta, \alpha < 1$ are constant parameters, $\lambda_{\min}(Q)$ is the minimal eigenvalue of Q, $L^2 = \eta^2 b_g^2 L_{\nabla\varphi}^2$.

Remark 3: 1) Since F is absent from (19)-(21) and (27), the prior knowledge of B and J is not needed; 2) Zeros can be assigned to the initial values of weights $\hat{W}$ without seeking an initially stable controller, which is a convenience in the industry. 3) As shown in Appendix B, when PMSM is stable, the numerator of (29) will be a positive number. 4) We can choose the smaller value of η to enhance the transient performance; however The smaller the value selected, the more the sampling number increases.

C. STABILITY ANALYSIS AND ELIMINATION OF ZENO PHENOMENON

The closed dynamics are stable through the analysis in the following theorem. Besides, the exclusion of the Zeno phenomenon is also analyzed to avoid the minimum interevent time reducing to zero, leading to the excessive increment of the cumulative events.

Theorem 3: For the current and speed tracking dynamics (9) with the drift parameters, the input constraints, and external disturbances. Let (27), (20), and (21) be the online weight update law, the ET optimal control, and ET disturbance compensation strategies, respectively. Let Assumptions 1, 2, Boundedness 1, Lemmas 1, 2, and Conditions 1, 2 be held. Then, the closed dynamics is asymptotically stable, and $\|\tilde{W}\| \ge b_{\tilde{W}}$, where $b_{\tilde{W}}$ is a boundary of a compact set. In addition, the Zeno phenomenon is excluded as the minimum interval between two successive events is greater than zero, i.e.,

$$t_{\min} = \min_k (t_{k+1} - t_k) \ge \frac{1}{\Gamma} \ln\left(1 + \min_{k\in\mathbb{N}} \frac{\|\underline{e}_T(t_{k+1}^-)\|}{\|\underline{z}\| + a}\right), \tag{30}$$

where Γ, a are positive bounds of system parameters.

Proof: See Appendix B. ■

TABLE 1. Nominal parameters of PMSM.

Parameters	Symbols	Units	Values
Rated Power	P_N	W	400
Rated Voltage	U_N	V	200
Rated Speed	n_N	rpm	3000
Permanent Magnet Flux	ψ_f	Wb	0.0615
Stator Resistance	R_s	Ω	2.7
Stator Inductance	L_d, L_q	mH	8.5
Nominal Inertia	J	kg$\cdot$ m^2	31.69×10^{-6}
Viscous Friction Coefficient	B	N$\cdot$ m$\cdot \frac{\text{s}}{\text{rad}}$	52.79×10^{-6}
Pole Pair	n_p		4
Encoder resolution		counts/rev	10 000

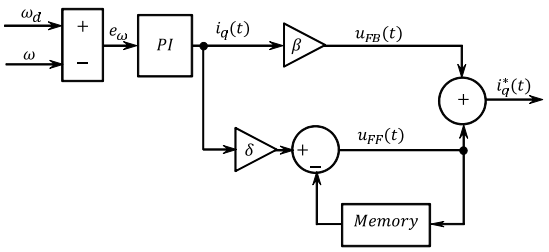

FIGURE 2. Structure of feedforward PI speed controller.

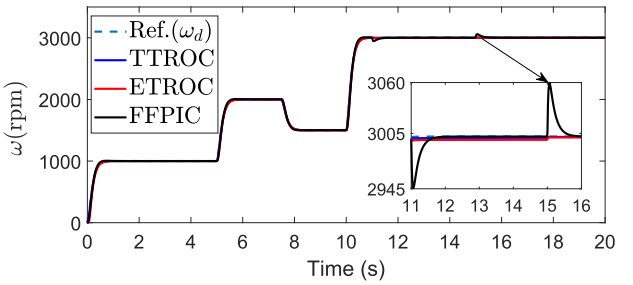

FIGURE 3. Speed tracking performance of ETROC, TTROC, FFPIC strategies.

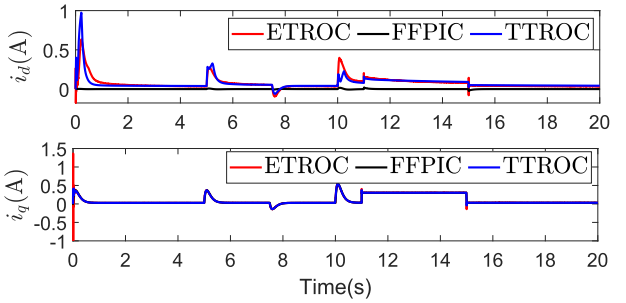

FIGURE 4. Currents i_{dq} of ETROC, TTROC, FFPIC strategies.

IV. SIMULATION AND EXPERIMENT

The ETROC strategy is verified in the section. Table 1 shows the nominal parameters of PMSM. The time-triggering robust optimal control (TTROC) strategy [17] and conventional PI control method are also used to compare with ETROC. The PI controller is reinforced with feedforward terms [30], namely feedforward-PI control (FFPIC).

In FFPIC, the feedforward term is employed for a simple learning scheme [30]. Fig. 2 shows the speed control structure, where u_{FF} is a feedforward term used to compensate the performance of u_{FB}. The control signal from the speed controller is presented by $i_q^* = u_{FB} + u_{FF}$, where

$$\begin{aligned} u_{FB} &= K_P^\omega(\omega_d - \omega) + K_I^\omega \int_0^t (\omega_d - \omega)d\tau \\ &= \beta\left(e_\omega + \gamma \int_0^t e_\omega d\tau\right) = \beta i_q, \end{aligned} \tag{31}$$

where $\beta = K_P^\omega$, $\gamma = K_I^\omega/\beta$. If the ratio $K_I^\omega/K_P^\omega \leq 1/\tau_r$, where τ_r is the desired closed-loop time constant, the best tuning for the PI speed controller is obtained [31]. For the motor ESTUN EMJ-04APB22, the well-tuned gains are $K_P^\omega = 0.1$, $K_I^\omega = 0.16$ with $\tau_r = 50$ms [31]. The parameter γ holds the following [Corollary 3.2] [30]:

$$\gamma \geq k_2 = \frac{B}{J} = \frac{52.79 \times 10^{-6}}{31.69 \times 10^{-6}}. \tag{32}$$

By employing the pass data, the simple update rule for u_{FF} is proposed as [30]

$$u_{FF} = \delta i_q - u_{FF}(t - T), \tag{33}$$

where $T = nT_s$, T_s is sampling time, $u_{FF}(t) = 0, \forall t \in [-T, 0]$. One can select $\delta = 0.2$ such that $\delta \leq 2\beta$. $T_s = 0.1$ms, $n = 1$ [Corollary 3.2] [30].

The feedforward control signals for the inner loop are defined as [31] and [32]

$$\begin{cases} u_d = -K_P^d i_d - K_I^d \int_0^t i_d d\tau - n_p \omega L_q i_q, \\ u_q = K_P^q(i_q^* - i_q) + K_I^q \int_0^t (i_q^* - i_q)d\tau + n_p \omega(L_d i_d + \psi_f). \end{cases}$$

The control gains are adjusted by $K_P^d = L_d w_{ci}$, $K_P^q = L_q w_{ci}$, $K_I^d = K_I^q = R_s w_{ci}$ [31], [32], where w_{ci} is the cut-off frequencies in the current loop. Considering closed-loop transfer functions from i_q^* and i_d^* to i_q and i_d as follows

$$G_{i_d}(s) = \frac{\omega_{ci}}{s + \omega_{ci}}, G_{i_q}(s) = \frac{\omega_{ci}}{s + \omega_{ci}}, \tag{34}$$

where s is the Laplace variable, the PI gains are tuned such that when w_{ci} is sufficiently high, $G_{i_d}(s) \approx 1 : i_d \to i_d^*$ and $G_{i_d}(s) \approx 1 : i_q \to i_q^*$. To this end, after tuned, the gains with the parameters of the motor ESTUN EMJ-04APB22 become $K_P^d = K_P^q = 60$, $K_I^d = K_I^q = 6000$ [31].

A. SIMULATION

In the simulation, disturbances are set $d_d = d_q = 0$, $d_\omega = 1$N·m, $d_\omega = 0$ at $t = 11$s and $t = 15$s, respectively. For ETROC and TTROC, the weight matrices (10) are $Q \in \mathbb{I}^{3\times3}$, $R \in \mathbb{I}^{4\times4}$. Approximator parameters are $\varphi(z) = [z_\omega^2, z_\omega z_{i_d}, z_\omega z_{i_q}, z_{i_d}^2, z_{i_d} z_{i_q}, z_{i_q}^2]^\top$, $\hat{W}(0) = 0$, $\beta = 25$. The stack size $P = 6$, $T = T_s$. $\chi = 1$, $\gamma = 10$, $\eta = 0.8$, $\alpha = 0.2$.

The speed tracking performance is shown in Fig. 3. Although ETROC, TTROC, and FFPIC can learn and give near-zero steady-state tracking errors, ETROC and TTROC can reject sudden torque disturbances compared to FFPIC. The current i_qs in Fig. 4 for three strategies are the same, but i_ds are different when dealing with the torque changes. The

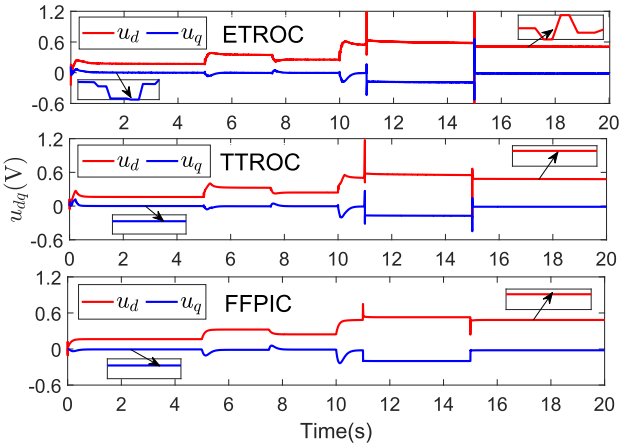

FIGURE 5. Control inputs u_{dq} of ETROC, TTROC, FFPIC strategies.

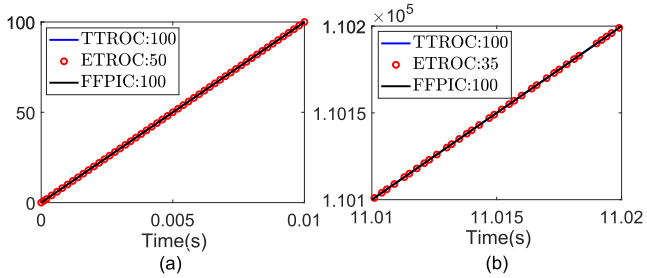

FIGURE 6. Number of events of ETROC, TTROC, FFPIC strategies: a) In the first stage; b) In the time of torque change.

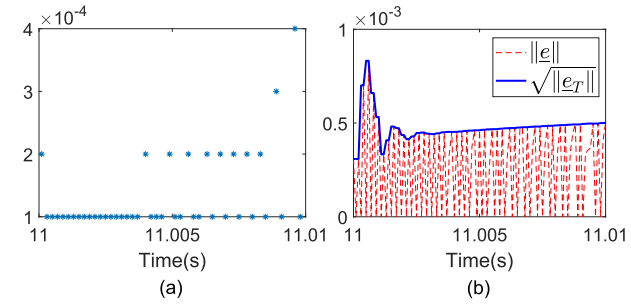

FIGURE 7. ETROC at the time of a torque change: a) Sampling period; b) Triggering error and threshold.

control voltages u_d and u_q in Fig. 5 show that ETROC and TTROC address the saturation as desired. Figs. 6 and 7 show that the ETROC strategy only updates its control parameters at some sampling times (events), but not at the entire sampling times as in TTROC and FFPIC. For example, within 20s, the number of events in TTROC or FFPIC is $20 \times 10^4 = 200.000$, while that in ETROC is 65.480. Fig. 7 also shows that the triggering error of ETROC is always below the square root of the triggering threshold. This means that the proposed event-triggering condition (29) is appropriate.

B. EXPERIMENT

Figure 8 shows an experimental prototype, where the commercial PMSM ESTUN EMJ-04APB22 is chosen and the kit of Texas Instrument TMDSHVMTRPFCKIT (High voltage motor control and power factor correction developer's

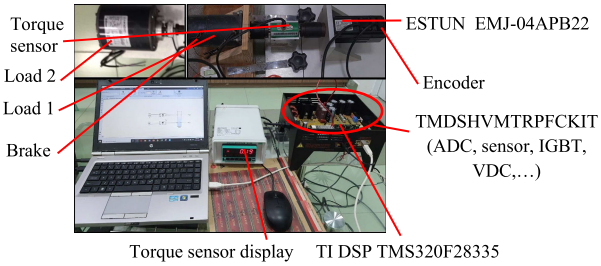

FIGURE 8. Experimental prototype.

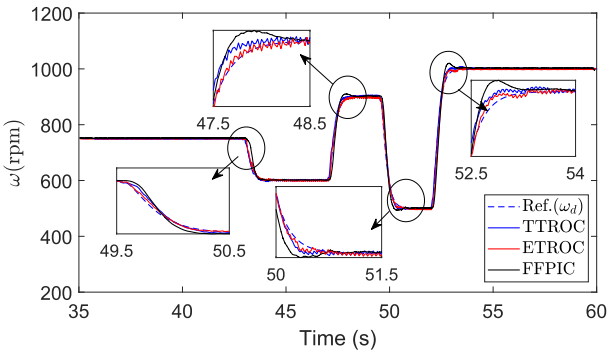

FIGURE 9. Speed tracking performances of ETROC, TTROC, FFPIC.

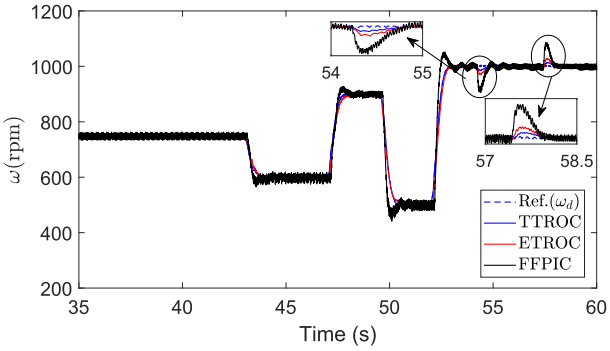

FIGURE 10. Speed tracking performances with coupled load and disturbance.

kit) with DSP TMS320F28335 is used to build control schemes. The embedded algorithm inside the DSP converts currents from the $\alpha\beta$-axes to the dq-axes for feedback through the Park-Clarke transform (Fig. 1) with the sampling period Ts $= 100\mu$s. It also converts the inverter phase voltages in $\alpha\beta$-axes from the voltages in the dq-axes using the inverse Park transform. Then, the actual voltages for controlling PMSM are obtained utilising the space vector modulation (SVM) method with switching frequency of 10kHz. The online data from the DSP is sent to Simulink of Matlab by the serial communications interface (SCI) after 35s. All converging parameters of the algorithm in the simulation are continued use for the embedded controller. The test load is two inductive motors in series and the load torque disturbance is applied to the PMSM through an electromagnetic brake attached to load motor 1.

In the case of separation between load motors 1 and 2, the speed tracking control performances of TTROC, ETROC,

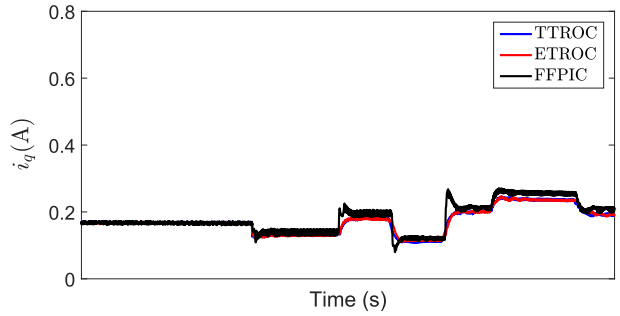

FIGURE 11. Currents in *q*-axis in experiment.

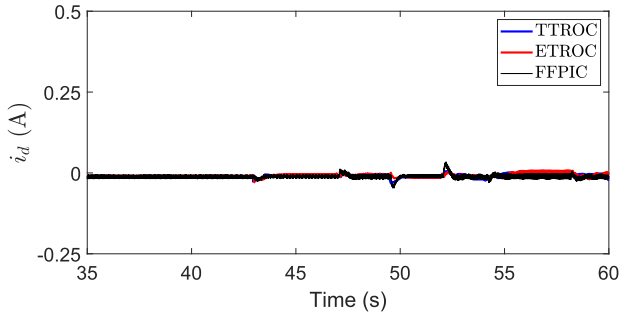

FIGURE 12. Currents in *d*-axis in experiment.

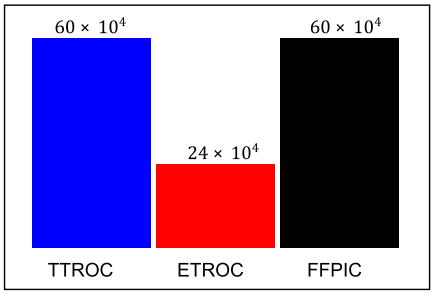

FIGURE 13. Comparison of triggering numbers among control methods.

and FFPIC are presented in Fig. 9. It can be seen that the tracking control performance of TTROC and ETROC is not much different and is better than that of FFPIC. However, the event number of 78.150 for ETROC using condition (29) is significantly smaller than that for TTROC with 200.000 events.

Figure 10 shows the speed tracking control performance of TTROC, ETROC, and FFPIC in the case of connection between motor loads 1 and 2. The tracking performance of TTROC and ETROC is still robust compared to the case of no connection. Meanwhile, the tracking performance of FFPIC fluctuates a lot because it cannot attenuate torque disturbance, especially at the time when the brake closes and opens to generate and release the torque of 1.5 N·m, respectively.

Correspondingly, Figs. 11 and 12 present the currents in the *dq*-axes reference frame. The forms of change in the experiment are consistent with the rules of speed change and load disturbance.

The statistics of the number of updating parameters and sending signals to the PMSM from the controllers are shown in Fig. 13. It can be seen that the triggering number of the proposed controller is much smaller than that of the other two. Of course, the Zeno behavior is not violated since the minimum triggering intervals are positive.

V. CONCLUSION

This paper has employed the event-triggering mechanism for an ET-robust optimal control strategy applied to PMSM drives with drift parameters, constrained inputs, and disturbances in current and speed dynamics. The objective is to optimize the cost function and mitigate the burden of communication resources and computational bandwidth between the controller and PMSM. The PMSM model is presented as a strict-feedback nonlinear system, and the ET-feedforward control strategy is introduced to transform the cascaded loops into an augmented system. The approximation of the ET control strategies is implemented via ADP and zero-sum game theory, which remove the knowledge of partially unknown dynamics and the PE condition. The exclusion of the Zeno phenomenon is also guaranteed by the proposed event-triggering condition. Developing distributed control strategies for multi-PMSM drives will be researched in future works.

APPENDIX A
PROOF OF LEMMA 1

Proof: Consider the Lyapunov function:

$$\mathcal{L}_1 = \frac{1}{2}\left(z_\omega^\top z_\omega + z_i^\top z_i\right). \tag{35}$$

Take the time derivative of (35) along with (1) using (2)-(5):

$$\begin{aligned}\dot{\mathcal{L}}_1 = &-\sum_{h=\omega,i} \chi z_h^\top \underline{z}_h + \sum_{h=\omega,i} z_h^\top g_h z_{h+1} \\ &+ \begin{bmatrix} z_\omega \\ z_i \end{bmatrix}^\top \left(\begin{bmatrix} f_\omega \\ f_i \end{bmatrix} + \begin{bmatrix} g_\omega & 0_{1\times 2} \\ 0_{2\times 2} & g_i \end{bmatrix} \begin{bmatrix} \underline{x}_i^\star \\ \underline{v}^\star \end{bmatrix} \right. \\ &\left. + \begin{bmatrix} k_\omega & 0_{1\times 2} \\ 0_{2\times 1} & \mathrm{I}_{2\times 2} \end{bmatrix} \begin{bmatrix} d_\omega \\ d_i \end{bmatrix} \right),\end{aligned} \tag{36}$$

where $z_{\omega+1} = z_i$ and $z_{i+1} = 0$. From (3) and (2) we have $\underline{z} = z(t_k)$, $e_h = z_h(t) - \underline{z}_h$, $t_k \le t < t_{k+1}$, $h = \omega, i$. Then, the first term of (36) can be written as

$$-\sum_{h=\omega,i} \chi z_h^\top \underline{z}_h = -\sum_{h=\omega,i} \chi z_h^\top z_h + \sum_{h=\omega,i} \chi z_h^\top e_h. \tag{37}$$

The second term in (36) is transformed as

$$\begin{aligned}\sum_{h=\omega,i} 2z_h^\top g_h z_{h+1} &\le \sum_{h=\omega,i} z_h^\top \|g_h\| z_h + \sum_{h=\omega,i} z_{h+1}^\top \|g_h\| z_{h+1} \\ &\le \sum_{h=\omega,i} 2z_h^\top \|g_h\| z_h.\end{aligned} \tag{38}$$

Substituting (37), (38) into (36) with noting (6) and (9) yields

$$\begin{aligned}\dot{\mathcal{L}}_1 &= z^\top \left(F + G\underline{u}^\star + Kd\right) - \sum_{h=\omega,i} \left(\chi(1-\kappa) - b_{gg}\right) \|z_h\|^2 \\ &\le z^\top \left(F + G\underline{u}^\star + Kd\right),\end{aligned} \tag{39}$$

where $b_{gg} = b_g - \frac{1}{4}$. For (7) we choose a Lyapunov function candidate:

$$\mathcal{L}_2 = \frac{1}{2}\left(z_\omega^\top z_\omega + z_i^\top z_i\right). \tag{40}$$

Taking derivative $\mathcal{J}_2$ along with (7) with noting (9), one has

$$\dot{\mathcal{L}}_2 = z^\top\left(F + G\underline{u}^\star + Kd\right). \tag{41}$$

It can be concluded that if we design control strategies to stabilize the closed dynamics of the augmented systems (7) and (9) are negative, so does (39). According to [21], the UUB of tracking error is guaranteed.

This completes the proof. ■

APPENDIX B
PROOF OF THEOREM 1

Proof: The proof is divided into two cases: the system within inter-events and at event-triggering instants. First, the following Lyapunov candidate is considered

$$\mathcal{L} = \underbrace{\int_{t-T}^{T}\mathcal{J}^\star(z)\mathrm{d}\tau}_{\mathcal{L}_1} + \underbrace{\frac{1}{2}\int_{t-T}^{T}\tilde{W}^\top\tilde{W}\mathrm{d}\tau}_{\mathcal{L}_2} + \underbrace{\mathcal{J}^\star(\underline{z})}_{\mathcal{L}_3}. \tag{42}$$

Case 1: as $\mathcal{J}^\star(\underline{z})$ is constant, $\dot{\mathcal{L}}_3 = 0$. Taking the derivative of L_1 along $\dot{z}$ from (22) when using $\nabla\mathcal{J}^\star(z)F$ from (16), one obtains

$$\dot{\mathcal{L}}_1 = \int_{t-T}^{T}\Big(-\nabla\mathcal{J}^{\star\top}\left(Gu^\star + Kd^\star\right) - z^\top Qz - U(u^\star) + \gamma^2 d^{\star\top}d^\star + \nabla\mathcal{J}^{\star\top}\left(G\hat{u} + K\hat{d}\right)\Big)\mathrm{d}\tau. \tag{43}$$

Replacing $u^\star$ from (15) to (11) yields

$$U(u^\star) = \eta(\nabla\mathcal{J}^\star)^\top G\tanh\left(\frac{1}{2\eta}R^{-1}G^\top\nabla\mathcal{J}^\star\right) + \eta^2\bar{R}\ln\left(\bar{\mathbf{1}} - \tanh^2\left(\frac{1}{2\eta}R^{-1}G^\top\nabla\mathcal{J}^\star\right)\right), \tag{44}$$

where $\bar{\mathbf{1}} = [1,1,1,1]^\top$, and $\bar{R}$ is a diagonal element vector of R. Replacing (15) into (44) obtains

$$\dot{\mathcal{L}}_1 = \int_{t-T}^{T}\Big(-z^\top Qz + \gamma^2\underline{d}^{\star\top}\underline{d}^\star - \eta^2\bar{R}\ln\left(\bar{\mathbf{1}} - \tanh^2(N^\star)\right) + \nabla\mathcal{J}^{\star\top}\left(G\underline{\hat{u}} + K\underline{\hat{d}} - Kd^\star\right)\Big)\mathrm{d}\tau. \tag{45}$$

The terms in (45) can be transformed to

$$\eta\bar{R}\ln\left(\bar{\mathbf{1}} - \tanh^2(M^\star)\right) = U(\underline{\hat{u}}) - \eta\nabla\mathcal{J}^{\star\top}G\tanh(M^\star) + \int_{\underline{\hat{u}}}^{u^\star}2\eta\tanh^{-T}(s/\eta)R\mathrm{d}s, \tag{46}$$

$$\nabla\mathcal{J}^{\star\top}G\underline{\hat{u}} = -\eta\nabla\mathcal{J}^{\star\top}G\tanh(N^\star) + \int_{u^\star}^{\underline{\hat{u}}}2\eta M^{\star\top}R\mathrm{d}s, \tag{47}$$

$$K^\top\nabla\mathcal{J}^{\star\top} = 2\gamma^2 d^{\star\top}, 2\gamma^2 d^{\star\top}\underline{\hat{d}} \le \gamma^2\|d^\star\|^2 + \gamma^2\|\underline{\hat{d}}\|^2, \tag{48}$$

$$z^\top Qz = \underline{z}^\top Q\underline{z} - 2\underline{z}^\top Q\underline{e} + \underline{e}^\top Q\underline{e} \ge (1-\eta)\underline{z}^\top\lambda_{\min}(Q)\underline{z} - \left(\frac{1}{\eta} - 1\right)\underline{e}^\top\lambda_{\min}(Q)\underline{e}. \tag{49}$$

Substituting (46)-(49) into (45) yields

$$\dot{\mathcal{L}}_1 \le \int_{t-T}^{T}\Big(-(1-\eta)\lambda_{\min}(Q)\|\underline{z}\|^2 + \left(\frac{1}{\eta} - 1\right)\lambda_{\min}(Q)\|\underline{e}\|^2 - U(\underline{\hat{u}}) - \varpi + \gamma^2\|\underline{\hat{d}}\|^2\Big)\mathrm{d}\tau, \tag{50}$$

where

$$\varpi = \int_{u^\star}^{\underline{\hat{u}}}2\eta\left(\tanh^{-1}(p/\eta) + M^\star\right)^\top R\mathrm{d}p. \tag{51}$$

Transforming $p = -\eta\tanh(\nu)$ yields

$$\varpi \le \int_{M^\star}^{\underline{\hat{M}}}2\eta^2\left(\nu - M^\star\right)^\top R\mathrm{d}\nu = \eta^2\left(\underline{\hat{M}} - M^\star\right)^\top R\left(\underline{\hat{M}} - M^\star\right) \le \eta^2\|R\|\|\underline{\hat{M}} - M^\star\|^2. \tag{52}$$

Adopting $\nabla\mathcal{J}^\star$ from (17) for $M^\star$ in (15) and replacing $M^\star$ and $\underline{\hat{M}}$ from (20) into (52), one obtains

$$\xi \le \frac{1}{2}\eta^2\|R\|\left\|R^{-1}\right\|^2\Big(\left\|G^\top\nabla\varphi^\top(\underline{z}) - G^\top\nabla\varphi_i^\top(z)\right\|^2\left\|\hat{W}\right\|^2 + \left\|G^\top\nabla\varphi_i^\top(z)\left(\tilde{W} + \nabla\varepsilon(z)\right)\right\|^2\Big). \tag{53}$$

Using an inequality form $(ab-cd)^2 \le 2a^2(b-d)^2 + 2d^2(a-c)^2$ and Assumptions 1, 2, Boundedness 1, one obtains

$$\begin{aligned}\left\|G^\top(\underline{x})\nabla\varphi^\top(\underline{z}) - G^\top(x)\nabla\varphi^\top(x)\right\|^2 &\le 2\left\|G(\underline{x})\right\|^2\left\|\nabla\varphi(\underline{z}) - \nabla\varphi(z)\right\|^2 + 2\left\|\nabla\varphi(z)\right\|^2\left\|G(\underline{x}) - G(x)\right\|^2\\ &\le 2b_g^2L_{\nabla\varphi}^2\|\underline{e}\|^2 + 4b_{\nabla\varphi}^2b_g^2.\end{aligned} \tag{54}$$

Substituting (53), (54) to (50), one has

$$\dot{\mathcal{L}}_1 \le \int_{t-T}^{T}\Big(-(1-\eta)\lambda_{\min}(Q)\|\underline{z}\|^2 - U(\underline{\hat{u}}) + \gamma^2\|\underline{\hat{d}}\|^2 + \left(\left(\frac{1}{\eta} - 1\right)\lambda_{\min}(Q) + L^2\left\|R^{-1}\right\|\left\|\hat{W}\right\|^2\right)\|\underline{e}\|^2 + \mu_1\left\|\tilde{W}\right\|^2 + \mu_2\|\tilde{W}\| + \lambda_1\Big)\mathrm{d}\tau, \tag{55}$$

where $\mu_1 = \eta^2 b_g^2 b_{\nabla\varphi}^2 \|R^{-1}\|$, $\mu_2 = \mu_1^2 b_{\nabla\varepsilon}^2 \|R^{-1}\|$, $\lambda_1 = 2b_{\nabla\varphi}^2 b_g^2$, $L^2 = \eta^2 b_g^2 L_{\nabla\varphi}^2$. Take differential L_2 along (28):

$$\dot{\mathcal{L}}_2 = \int_{t-T}^{t} \Big(-\beta \tilde{W}^\top \Omega \tilde{W} + \beta \tilde{W}^\top \Big(\Delta\varphi \varepsilon_H + \sum_{l=1}^{P} \Delta\varphi(t_l)\varepsilon_H(t_l) \Big) \Big) \mathrm{d}\tau, \tag{56}$$

where $\Omega = \Delta\varphi\Delta\varphi^\top + \sum_{l=1}^{P} \Delta\varphi(t_l)\Delta\varphi(t_l)^\top$, $\Omega > 0$. Using the upper bound of $\varepsilon_H(.)$, the Young's inequality and Condition 1 for (56) yields

$$\dot{\mathcal{L}}_2 \leq -(\beta-1)\lambda_{\min}(\Omega) \int_{t-T}^{t} \left\|\tilde{W}\right\|^2 \mathrm{d}\tau + \frac{\beta^2}{4}(P+1) \int_{t-T}^{t} b_{\varepsilon H}^2 \mathrm{d}\tau. \tag{57}$$

Substituting (57) and (55) to (42) yields

$$\dot{\mathcal{L}} \leq \int_{t-T}^{t} \Big(-(1-\eta)\lambda_{\min}(Q)\|\underline{z}\|^2 - U(\underline{\hat{u}}) + \gamma^2 \|\underline{\hat{d}}\|^2 + \Big(\Big(\frac{1}{\eta} - 1\Big)\lambda_{\min}(Q) + L^2 \|R^{-1}\| \|\hat{W}\|^2 \Big) \|\underline{e}\|^2 - \mu_3 \Big(\|\tilde{W}\| - \frac{\mu_2}{2\mu_3} \Big)^2 + \lambda_2 \Big) d\tau \tag{58}$$

where $\mu_3 = \beta - \mu_1 - 1$. If $\beta > \mu_1 + 1$ then $\mu_3 > 0$, $\lambda_2 = \lambda_1 + \frac{\beta^2}{4}(P+1)b_{\varepsilon H}^2 + \frac{\mu_2^2}{4\mu_3}$. Define $b_{\tilde{W}} = \sqrt{\lambda_2/\mu_3} + \frac{\mu_2}{2\mu_3}$ and apply the triggering condition 2, we have $\dot{L} < -\frac{1}{T}\alpha((1-\eta)\lambda_{\min}(Q)\|\underline{z}\|^2 + U(\underline{\hat{u}}) - \gamma^2\|\underline{\hat{d}}\|^2) \leq 0$, $\forall t$. The closed dynamics is stabilized asymptotically, and the UUB of approximation dynamics is guaranteed.

Case 2: Consider the system is at $\forall t = t_k, \forall k \in \mathbb{N}$, taking the difference of (42) we have

$$\Delta\mathcal{L} = \mathcal{J}^\star(\underline{z}(t_k)) - \mathcal{J}^\star(\underline{z}(t_{k-1})) + \int_{t_k-T}^{t_k} \mathcal{J}^\star(\underline{z})\mathrm{d}\tau - \int_{t_k^- - T}^{t_k^-} \mathcal{J}^\star(z(t^-))\mathrm{d}\tau + \frac{1}{2}\tilde{W}^\top(t_k)\tilde{W}(t_k) - \frac{1}{2}\tilde{W}^\top(t^-)\tilde{W}(t^-). \tag{59}$$

From (58), since $\dot{\mathcal{L}} < 0$, the state of (9) and (17) are continuous, one has

$$\int_{t_k-T}^{t_k} \mathcal{J}^\star(\underline{z}(t_k))d\tau \leq \int_{t_k^- - T}^{t_k^-} \mathcal{J}^\star(z(t^-))\mathrm{d}\tau \tag{60}$$

$$\tilde{W}^\top(t_k)\tilde{W}(t_k) \leq \tilde{W}^\top(t^-)\tilde{W}(t^-). \tag{61}$$

Then, we rewrite $\Delta\mathcal{L}$ as

$$\Delta\mathcal{L} \leq \mathcal{J}^\star(\underline{z}(t_k)) - \mathcal{J}^\star(\underline{z}(t_{k-1})) \leq \mathcal{J}^\star(z(t^-)) - \mathcal{J}^\star(\underline{z}(t_{k-1})) \leq -\psi\|z(t^-) - \underline{z}(t_{k-1})\| = -\psi\|\underline{e}(t_{k-1})\|, \tag{62}$$

where ψ is within a class-κ function [21]. Recalling (59), it can be seen that the (42) is still decreasing at $t = t_k$, $k \in \mathbb{N}$. Synthesizing (58) and (62), the asymptomatic stability is guaranteed.

Next, let us note the boundedness of (20) and (21) and and the Lipschitz property of F to prove the minimum interval between two successive events is greater than zero. The dynamics (9), $\forall t \in [t_k, t_{k+1})$, satisfies

$$\|\dot{z}\| \leq b_f\|z\| + \Gamma_0\|\hat{W}\|\|\underline{z}\|, \tag{63}$$

where $\Gamma_0 = \|R^{-1}\|/2b_g^2 L_{\nabla z} + J_{\max}^2/(2\gamma^2)L_{\nabla z}$, $F \leq b_f\|z\|$, $b_f > 0$. Note that $\underline{e} = z - \underline{z}$, with a small positive real number a, $\Gamma = \Gamma_0 + b_f$ we have

$$\|\dot{\underline{e}}\| \leq \Gamma\|\underline{e}\| + \Gamma\Big(\|\underline{z}\| + a\Big). \tag{64}$$

Formally, the rest of the proof can follow from [8].

This completes the proof. ■

ACKNOWLEDGMENT

The authors acknowledge the Ho Chi Minh City University of Technology (HCMUT), VNU-HCM for supporting this study.

CONFLICT OF INTEREST

The authors declare no potential conflict of interests.

REFERENCES

[1] H. Li, B. Song, T. Chen, Y. Xie, and X. Zhou, "Adaptive fuzzy PI controller for permanent magnet synchronous motor drive based on predictive functional control," *J. Franklin Inst.*, vol. 358, no. 15, pp. 7333–7364, Oct. 2021.

[2] S. Cheng, J. Yu, L. Zhao, and Y. Ma, "Adaptive fuzzy control for permanent magnet synchronous motors considering input saturation in electric vehicle stochastic drive systems," *J. Franklin Inst.*, vol. 357, no. 13, pp. 8473–8490, Sep. 2020.

[3] S. Ding, Q. Hou, and H. Wang, "Disturbance-observer-based second-order sliding mode controller for speed control of PMSM drives," *IEEE Trans. Energy Convers.*, vol. 38, no. 1, pp. 100–110, Mar. 2023.

[4] V. Šmídl, Š. Janous, L. Adam, and Z. Peroutka, "Direct speed control of a PMSM drive using SDRE and convex constrained optimization," *IEEE Trans. Ind. Electron.*, vol. 65, no. 1, pp. 532–542, Jan. 2018.

[5] T. D. Do, H. H. Choi, and J.-W. Jung, "SDRE-based near optimal control system design for PM synchronous motor," *IEEE Trans. Ind. Electron.*, vol. 59, no. 11, pp. 4063–4074, Nov. 2012.

[6] P. Tabuada, "Event-triggered real-time scheduling of stabilizing control tasks," *IEEE Trans. Autom. Control*, vol. 52, no. 9, pp. 1680–1685, Sep. 2007.

[7] A. Sahoo, V. Narayanan, and S. Jagannathan, "A min–max approach to event- and self-triggered sampling and regulation of linear systems," *IEEE Trans. Ind. Electron.*, vol. 66, no. 7, pp. 5433–5440, Jul. 2019.

[8] Q. Zhang, D. Zhao, and Y. Zhu, "Event-triggered H_∞ control for continuous-time nonlinear system via concurrent learning," *IEEE Trans. Syst., Man, Cybern., Syst.*, vol. 47, no. 7, pp. 1071–1081, Jul. 2017.

[9] N. K. Dhar, N. K. Verma, and L. Behera, "Adaptive critic-based event-triggered control for HVAC system," *IEEE Trans. Ind. Informat.*, vol. 14, no. 1, pp. 178–188, Jan. 2018.

[10] X. Chen, X. Chen, W. Bai, and Z. Guo, "Event-triggered optimal control for macro-micro composite stage system via single-network ADP method," *IEEE Trans. Ind. Electron.*, vol. 68, no. 5, pp. 4190–4198, May 2021.

[11] T. Yang, N. Sun, H. Chen, and Y. Fang, "Adaptive optimal motion control of uncertain underactuated mechatronic systems with actuator constraints," *IEEE/ASME Trans. Mechatronics*, vol. 28, no. 1, pp. 210–222, Feb. 2023.

[12] M. Wang, L. Wang, R. Huang, and C. Yang, "Event-based disturbance compensation control for discrete-time SPMSM with mismatched disturbances," *Int. J. Syst. Sci.*, vol. 52, no. 4, pp. 785–804, Mar. 2021.

[13] S. Zhou, Y. Li, and S. Tong, "Finite-time adaptive neural network event-triggered output feedback control for PMSMs," *Neurocomputing*, vol. 533, pp. 10–21, May 2023.
[14] W. Li, Y. Liu, Y. Huang, H. Li, and F. Li, "Event-triggered position tracking for permanent magnet synchronous motor," in *Proc. Chin. Control Conf. (CCC)*, Jul. 2019, pp. 691–696.
[15] X. Cai, Z. Zhang, J. Wang, and R. Kennel, "Optimal control solutions for PMSM drives: A comparison study with experimental assessments," *IEEE J. Emerg. Sel. Topics Power Electron.*, vol. 6, no. 1, pp. 352–362, Mar. 2018.
[16] P. Krause, O. Wasynczuk, S. D. Sudhoff, and S. Pekarek, *Analysis of Electric Machinery and Drive Systems*. Hoboken, NJ, USA: Wiley, 2013.
[17] L. N. Tan and T. C. Pham, "Optimal tracking control for PMSM with partially unknown dynamics, saturation voltages, torque, and voltage disturbances," *IEEE Trans. Ind. Electron.*, vol. 69, no. 4, pp. 3481–3491, Apr. 2022.
[18] Y. Zhu, D. Zhao, H. He, and J. Ji, "Event-triggered optimal control for partially unknown constrained-input systems via adaptive dynamic programming," *IEEE Trans. Ind. Electron.*, vol. 64, no. 5, pp. 4101–4109, May 2017.
[19] K. G. Vamvoudakis, M. F. Miranda, and J. P. Hespanha, "Asymptotically stable adaptive-optimal control algorithm with saturating actuators and relaxed persistence of excitation," *IEEE Trans. Neural Netw. Learn. Syst.*, vol. 27, no. 11, pp. 2386–2398, Nov. 2016.
[20] M. De Soricellis, D. Da Ru, and S. Bolognani, "A robust current control based on proportional-integral observers for permanent magnet synchronous machines," *IEEE Trans. Ind. Appl.*, vol. 54, no. 2, pp. 1437–1447, Mar. 2018.
[21] H. K. Khalil, *Nonlinear Systems*. Upper Saddle River, NJ, USA: Prentice-Hall, 2002.
[22] H. Zargarzadeh, T. Dierks, and S. Jagannathan, "Optimal control of nonlinear continuous-time systems in strict-feedback form," *IEEE Trans. Neural Netw. Learn. Syst.*, vol. 26, no. 10, pp. 2535–2549, Oct. 2015.
[23] N. D. Dien, N. T. Luy, L. K. Lai, and T. T. Hai, "Optimal tracking control for robot manipulators with input constraint based reinforcement learning," *J. Comput. Sci. Cybern.*, vol. 39, no. 2, pp. 175–189, Jun. 2023.
[24] T. Basar and P. Bernhard, *H_∞ Optimal Control and Related Minimax Design Problems: A Dynamic Game Approach*, 2nd ed. Boston, MA, USA: Birkhauser, 1995.
[25] A. van der Schaft, "L_2-gain analysis of nonlinear systems and nonlinear state feedback H_∞ control," *IEEE Trans. Autom. Control*, vol. 37, no. 6, pp. 770–784, Jun. 1992.
[26] M. Abu-Khalaf and F. L. Lewis, "Nearly optimal control laws for nonlinear systems with saturating actuators using a neural network HJB approach," *Automatica*, vol. 41, no. 5, pp. 779–791, May 2005.
[27] B. A. Finlayson, *The Method of Weighted Residuals and Variational Principles*. New York, NY, USA: Academic Press, 1990.
[28] D. Vrabie and F. Lewis, "Neural network approach to continuous-time direct adaptive optimal control for partially unknown nonlinear systems," *Neural Netw.*, vol. 22, no. 3, pp. 237–246, Apr. 2009.
[29] G. Chowdhary and E. Johnson, "Concurrent learning for convergence in adaptive control without persistency of excitation," in *Proc. 49th IEEE Conf. Decis. Control (CDC)*, Dec. 2010, pp. 3674–3679.
[30] H. H. Choi, E. K. Kim, D. Y. Yu, J. W. Jung, and T. H. Kim, "Precise PI speed control of permanent magnet synchronous motor with a simple learning feedforward compensation," *Electr. Eng.*, vol. 99, no. 1, pp. 133–139, Mar. 2017.
[31] F. Mendoza-Mondragón, V. M. Hernández-Guzmán, and J. Rodríguez-Reséndiz, "Robust speed control of permanent magnet synchronous motors using two-degrees-of-freedom control," *IEEE Trans. Ind. Electron.*, vol. 65, no. 8, pp. 6099–6108, Aug. 2018.
[32] S.-K. Kim, "Robust adaptive speed regulator with self-tuning law for surfaced-mounted permanent magnet synchronous motor," *Control Eng. Pract.*, vol. 61, pp. 55–71, Apr. 2017.

LUY NGUYEN TAN (Senior Member, IEEE) received the B.S. and M.Sc. degrees in computer science and automation and control engineering and the Ph.D. degree in automation from the Ho Chi Minh City University of Technology (HCMUT), Vietnam, in 1996, 2006, and 2015, respectively.

He is currently with the Faculty of Electric-Electronics Engineering (FEEE), HCMUT, Vietnam National University Ho Chi Minh City (VNU-HCM), Vietnam. His current research interests include adaptive dynamic programming, distributed control, large-scale systems, and deep learning. He served as a Reviewer for many journals, including IEEE TRANSACTIONS ON NEURAL NETWORK AND LEARNING SYSTEMS, IEEE TRANSACTIONS ON INDUSTRIAL ELECTRONICS, IEEE TRANSACTIONS ON INDUSTRIAL INFORMATICS, IEEE TRANSACTIONS ON CYBERNETICS, IEEE TRANSACTIONS ON SYSTEMS, MAN CYBERNETICS: SYSTEMS, IEEE ACCESS, and Elsevier.

THANH PHAM CONG received the B.S. and M.Sc. degrees in automation and control engineering from the Ho Chi Minh City University of Technology, Ho Chi Minh City, Vietnam, in 2002 and 2006, respectively, and the Ph.D. degree from the Department of Control Science and Engineering, Huazhong University of Science and Technology (HUST), Wuhan, China, in 2014. He is currently with the Faculty of Aeronautical Electronics-Telecommunications, Vietnam Aviation Academy. His current research interests include ac motor, power electronics, and adaptive dynamic programming.

DUY PHAM CONG received the B.Eng. and M.Eng. degrees in electrical and electronics engineering from the Ho Chi Minh City University of Technology, Ho Chi Minh City, Vietnam, in 2001 and 2007, respectively, and the Ph.D. degree from Hunan University, China, in 2012. He is currently with the Faculty of Electrical Engineering Technology, Industrial University of Ho Chi Minh City, Vietnam. His research interests include power conversion, electrical machine, and advanced control techniques for electrical drives.